Electronic Supplementary Material (ESI) for RSC Advances.
This journal is © The Royal Society of Chemistry 2015

Supplementary information

Isolation and identification of *Bacillus licheniformis*

Thermophilic microbes are among the few extremophiles commonly found in the geothermal areas of the world, and particularly, the few hot springs of Saudi Arabian deserts [22]. The uniqueness of enzymatic activity responsible for their adaptation and survival at these extreme climatic conditions is related to well define biochemical pathways and DNA conformations. Some thermophiles of the *Thermus* and *Bacillus* genera have been reported to be resistant to extreme pH and salinity, as well as solvents [23, 24]. The global market and demands for possible cellular and biocatalytic applications have increased since the isolation and characterization of the first thermophilic bacterial strains by Miquel's group in 1888, in food processing, waste recycling, pharmaceutics and antifouling activities [25, 26]. In this work, the isolation of a thermophilic *B. licheniformis* strain (No. 6) and subsequent genotypic and phenotypic characterization is reported from the hot springs of the Gazan area (Lat. 43°15E', Long. 16°56N'), Eastern Province of Saudi Arabia. The collection of spring water samples, preservation and storing procedures employed in the work are similar to the ones previously reported by Khalil *et al.* [25, 27]. Appropriate volumes of sterile containers, buffers and media used for the inoculation and culturing procedures were carried out at recommended incubation temperatures and durations in line with this bacterial strain. Single *Bacillus* colonies from the culture were streaked and picked onto TT agar plates, and then incubated for 48 h with gentle stirring (300 rpm) at 55─70 °C. Distinctive colonies from the incubated TT agar were transferred and stored at ─80 °C in fresh glycerol in TT broth [25]. Labelled as *Bacillus* strain, the isolated wild type strain was identified by 16S rRNA gene PCR and sequencing at KFUPM, Saudi Arabia. Its gene alignment was compared with the closest GenBank match at the highest degree of confidence, and later confirmed as *Bacillus licheniformis*. The elaborate non-specific 16S rRNA gene PCR amplification procedure with appropriate oligonucleotide primers have been previously reported [25, 27].

Metal surface polishing procedure, chemical composition and SEM microstructure of mild steel

The mild steel substrate used in this work is a S─36 type grade specimen with the following chemical composition (wt.%): Mn 0.60, C 0.15, P 0.030, S 0.035 and the remaining percentage is allocated to Fe. To study the morphology of the substrate's microstructure, it was first mechanically cut into a 1 cm x 1 cm coupon and abraded with different grades of silicon carbide papers (between grit no. 120 and 800), repeatedly rinsed with absolutely ethanol before finally polished to mirror surface finish with micro-scaled alumina (gradually from 9 to 1 μm). Polishing was proceeded with acetone ultrasonication and later re-rinsed in the acetone and dried in warm air [29]. Figure S1 displays the SEM microstructure of S─36 mild steel grade imaged after sample polishing with relatively uniform distribution of phases. The SEM micrograph of this material displays predominantly areas rich in ferrite (bright patches) outlining the grain boundaries with those of pearlite (dark portion; a ferrite/cementite lamellar structure); typical of low carbon steel. The differences in the chemistries of these regions contribute to the corrosion of mild steel due to galvanic effect as ferrite is most likely to be affected since the cementite content of pearlite is more electrochemically stable. The elemental mapping of the microstructure by scanning electron microscopy-energy dispersive X-ray spectrometry (SEM-EDS) reveals trace composition of Mn 0.75%, C (0.20%), P and S (<0.2%) with remaining percentage being dominantly Fe (Figure S1). The C content in most ferrite-pearlite steel grades as well as their grain sizes determine their microstructure and resulting properties [49].

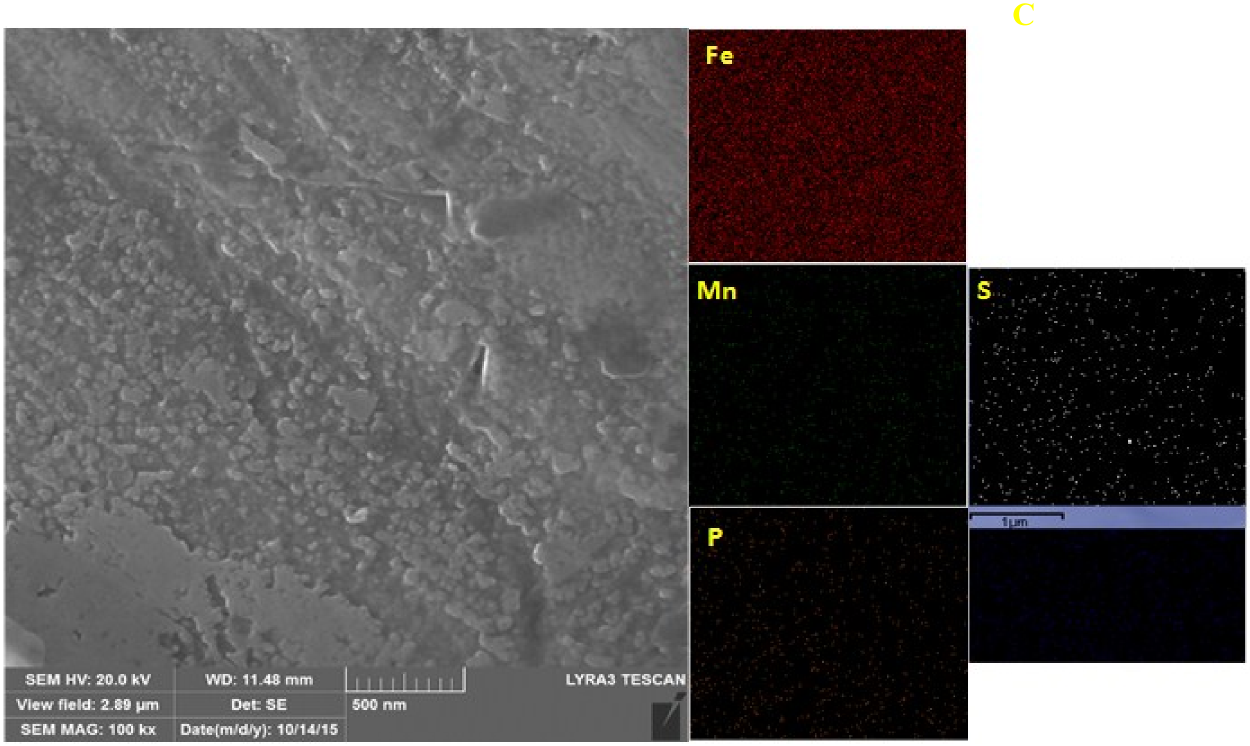

Figure S1. SEM micrographs of S─36 mild steel grade showing its microstructure (left panel; 500 nm); EDX mapping (right panel; all micrographs are equally scaled (1 µm)).

Map of area of fouling study

A field trial in a natural corrosive environment was conducted to ascertain the corrosion protection properties of the unmodified and the abiotic and bio-modified coating systems. The edges of the immersed S36 panels were covered with insulation tape leaving only a defined test area for fouling studies. The marine fouling studies were carried out in the hyper-saline seawater of the KFUPM beach, Half-Moon Bay, Al Khobar, Saudi Arabia, at ambient conditions (Figure S2). This beach is known for its slow moving waves along the Arabian Gulf at all seasons with high fouling activities and salinity. KFUPM Beach is a private section of the Half Moon Bay owned by KFUPM for recreation as well as research purposes. Generally, the bay has a record depth between 22 and 50 feet with very few shallow entrances; it is known for the presence of groupers that has been widely fished. The beach houses huge biodiversity ranging from floral to fauna and it is very saline due to the Gulf's high evaporation rate, humidity and hot climate. Table S1 presents the mean values of temperature, pH, and salinity of KFUPM Beach (at the point of sample immersion) recorded throughout the 10 week period of fouling studies.

Figure S2. KFUPM beach at Half Moon Bay, Al-Khobar, Saudi Arabia (source: Google map; Lat. 26°28', Long. 50°20').

Table S1: Mean values of temperature, pH, and salinity of KFUPM Beach (at the point of sample immersion) recorded throughout the 10 weeks of fouling studies.

Days	Temperature (^{o}C)	pH	*Salinity
Day of immersion	28.9 ±0.1	7.6±0.2	65.8±1.0
Week 2	27.2±0.2	7.4±0.2	67.5±1.2
Week 4	28.3±0.2	7.4±0.2	66.4±0.9
Week 6	29.2±0.3	7.8±0.3	71.0±0.6
Week 8	30.8±0.2	7.7±0.2	70.2±0.8
Week 10	29.0±0.2	7.3±0.3	71.2±0.7

Above parameters were taken in the early hours of the mornings; *Values of salinity kept increasing steadily as the hot Arabian summer approached in June; with salinity values more than 40 ppt, KFUPM beach could be classified as being "*hypersaline*".

Appearance of the coated steel substrates after curing

Figure 3 shows the appearance of the coated steel substrates after 24 hour curing at room temperature for each matrix; the coating appears evenly distributed on the steel surface with no signs of mechanical defects.

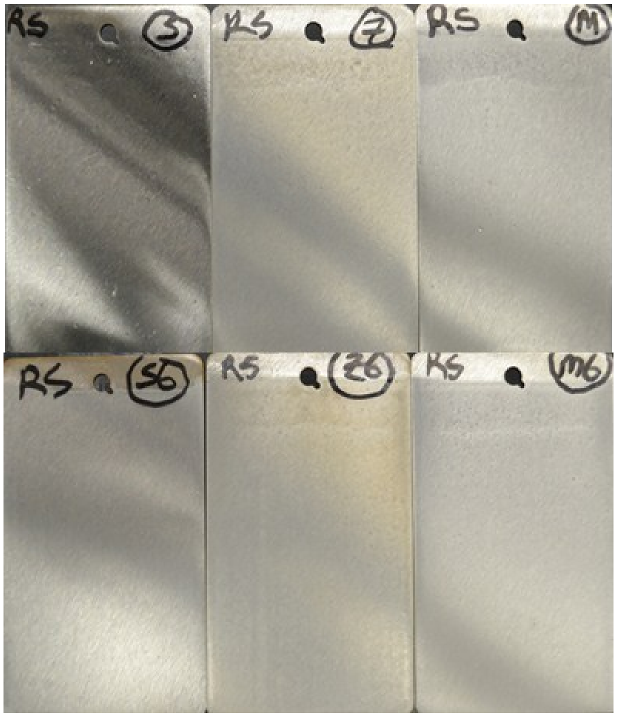

Figure S3. Mild steel Q panels (0.032”×3”×5”) coated with different functionalized sol-gel matrices.

Viability of B6 endospores in sol-gel coating systems

Viable (living) endospores were enumerated by plating diluted suspensions of the endospores from each bioactive coating system (50 μL of a 10^{-5} dilution) onto TT agar plates and incubated at 30 ^{o}C. Significant colony growth was observed in all bioactive samples demonstrating germination of the endospores to vegetative cells [16].

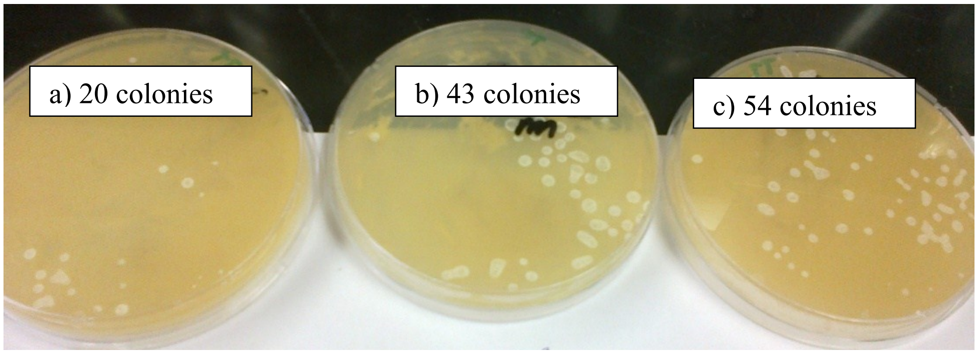

Figure S4. Growth of *B. licheniformis* strain No. 6 (B6) colonies from endospores in sol-gel coatings: a) Sol-gel encapsulated with B6 endospores (S6), b) Sol-gel encapsulated with MOLY and B6 endospores (SM6), c) Sol-gel encapsulated with ZAPP & B6 endospores (SZ6).

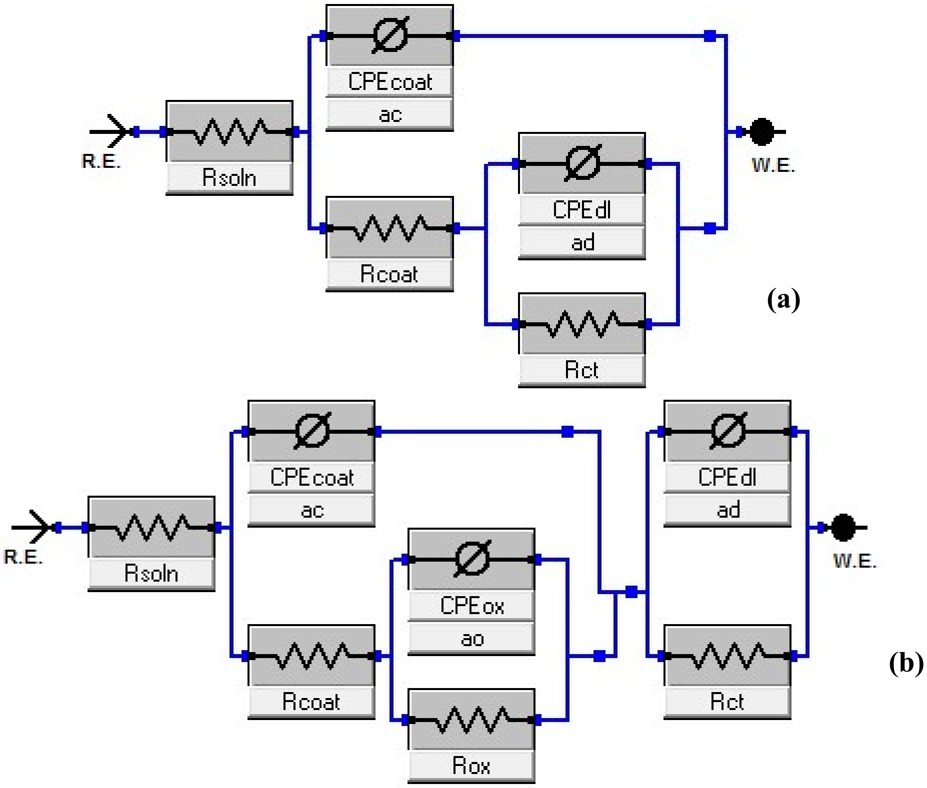

Figure S5. Equivalent circuit models used in fitting experimental data by Simplex method; adopted from Garmy EChem Analyst software's model editor. Two-time and three-time constant equivalent circuit models, as presented in Figure S5, are allotted to respective coating matrices for the fitting and analyzing of the experimental impedance data, with each model selected based on the respective contributions of coating systems at a particular immersion period. The electrochemical parameters derived for these circuit models are listed in the Supplementary information (Table S2) for each coating matrix.

Table S2 (a). Variation of *EIS parameters for abiotic sol-gel coated steel electrode immersed in 3.5 wt% NaCl at room temperature at different exposure periods.

(S)	**24 HOURS**	**48 HOURS**	**72 HOURS**	**96 HOURS**	**120 HOURS**	**144 HOURS**	**WEEK 1**	**WEEK 2**
R_{soln} (mΩ)	10.00	10.00	10.00	10.00	10.00	10.00	10.00	10.00
R_{coat} (kΩ)	5.850	5.769	4.158	3.451	2.964	2.809	2.142	2.006
CPE_{coat} (Y_o, nF cm^{-2} $s^{-(1-\alpha c)}$)	3.656	9.069	10.324	13.79	12.799	15.065	18.752	19.99
a_c	0.952	0.952	0.906	0.952	0.952	0.952	0.952	0.952
R_{ct} (kΩ)	67	38	29.65	15.28	15.90	10.63	7.94	9.48
CPE_{dl} (Y_o, µF cm^{-2} $s^{-(1-\alpha c)}$)	21.43	25.98	27.81	35.11	38.38	74.68	78.74	95.50
a_d	0.952	0.952	0.952	0.952	0.952	0.952	0.952	0.952
CIRCUIT TYPE	**R(Q(R(QR)))**	**R(Q(R(QR)))**	**R(Q(R(QR)))**	**R(Q(R(QR)))**	**R(Q(R(QR)))**	**R(Q(R(QR)))**	**R(Q(R(QR)))**	**R(Q(R(QR)))**

(SZ)	**24 HOURS**	**48 HOURS**	**72 HOURS**	**96 HOURS**	**120 HOURS**	**144 HOURS**	**WEEK 1**	**WEEK 2**
R_{soln} (mΩ)	10.00	10.00	10.00	10.00	10.00	10.00	10.00	10.00
R_{coat} (kΩ)	19.90	10.30	9.502	8.762	8.358	6.512	6.319	4.982
CPE_{coat} (Y_o, nF cm^{-2} $s^{-(1-\alpha c)}$)	3.0066	5.512	6.13	7.484	6.887	8.795	10.266	11.347
a_c	0.952	0.968	0.944	0.933	0.952	0.952	0.952	0.952
R_{ox} (kΩ)	—	—	68.86	52.57	28.73	14.592	8.134	7.148
CPE_{ox} (Y_o, µF cm^{-2} $s^{-(1-\alpha c)}$)	—	—	36.49	44.06	86.07	107.6	134.13	136.73
a_o	—	—	0.275	0.256	0.403	0.426	0.531	0.582
R_{ct} (kΩ)	86.4	40.38	31.26	31.51	16.78	12.732	8.76	12.81
CPE_{dl} (Y_o, µF cm^{-2} $s^{-(1-\alpha c)}$)	12.83	21.75	25.13	33.09	34.23	46.3	50.6	55.00
a_d	0.952	0.952	0.813	0.828	0.952	0.952	0.952	0.952
CIRCUIT TYPE	**R(Q(R(QR)))**	**R(Q(R(QR)))**	**R(Q(R(QR)))(QR)**	**R(Q(R(QR)))(QR)**	**R(Q(R(QR)))(QR)**	**R(Q(R(QR)))(QR)**	**R(Q(R(QR)))(QR)**	**R(Q(R(QR)))(QR)**

(SM)	**24 HOURS**	**48 HOURS**	**72 HOURS**	**96 HOURS**	**120 HOURS**	**144 HOURS**	**WEEK 1**	**WEEK 2**
R_{soln} (mΩ)	10.00	10.00	10.00	10.00	10.00	10.00	10.00	10.00
R_{coat} (kΩ)	52.64	23.46	14.25	14.34	9.587	8.920	6.794	5.003
CPE_{coat} (Y_o, nF cm^{-2} $s^{-(1-\alpha c)}$)	2.502	2.848	3	4.550	3.652	3.113	5.260	7.41
a_c	0.925	0.952	0.952	0.952	0.966	0.952	0.952	0.952
R_{ox} (kΩ)	–	–	76.7	58.2	36.306	21.815	16.8	16.04
CPE_{ox} (Y_o, µF cm^{-2} $s^{-(1-\alpha c)}$)	–	–	21.98	19.20	25.36	5.69	116.4	127.1
a_o	–	–	0.92	0.92	0.92	0.92	0.92	0.92
R_{ct} (kΩ)	112.92	52	40.33	35.61	26.48	18.74	10.902	25.87
CPE_{dl} (Y_o, µF cm^{-2} $s^{-(1-\alpha c)}$)	12.02	19.69	20	31.00	31.95	35.14	39.65	40
a_d	0.952	0.952	0.948	0.952	0.952	0.952	0.952	0.786
CIRCUIT TYPE	**R(Q(R(QR)))**	**R(Q(R(QR)))**	**R(Q(R(QR)))(QR)**	**R(Q(R(QR)))(QR)**	**R(Q(R(QR)))(QR)**	**R(Q(R(QR)))(QR)**	**R(Q(R(QR)))(QR)**	**R(Q(R(QR)))(QR)**

*Data were collected by fitting experimental impedance results with electrical circuit models by Simplex method.

Table S2 (b). Variation of EIS parameters for biotic sol-gel (S) coated steel electrode immersed in 3.5 wt% NaCl at room temperature at different exposure periods.

(S6)	**24 HOURS**	**48 HOURS**	**72 HOURS**	**96 HOURS**	**120 HOURS**	**144 HOURS**	**WEEK 1**	**WEEK 2**
R_{soln} (mΩ)	10.00	10.00	10.00	10.00	10.00	10.00	10.00	10.00
R_{coat} (kΩ)	17.96	9.446	7.261	7.921	7.848	7.574	5.224	4.327
CPE_{coat} (Y_o, nF cm^{-2} $s^{-(1-\alpha c)}$)	1.813	1.346	1.592	1.931	2.0915	2.0913	3	4
a_c	0.952	0.952	0.868	0.952	0.845	0.952	0.952	0.952
R_{ox} (kΩ)	–	–	75.88	66.597	54.25	44.82	31.77	15.48
CPE_{ox} (Y_o, µF cm^{-2} $s^{-(1-\alpha c)}$)	–	–	8.544	15.53	17	29.253	55.33	86.47
a_o	–	–	0.952	0.952	0.853	0.952	0.952	0.952
R_{ct} (kΩ)	135.3	68.11	45.650	35.99	22.80	18.33	14.73	11.22
CPE_{dl} (Y_o, µF cm^{-2} $s^{-(1-\alpha c)}$)	12.863	18.074	19	20.4	28.98	31.79	33	39
a_d	0.583	0.464	0.1000	0.342	0.320	0.519	0.162	0.1000
CIRCUIT TYPE	**R(Q(R(QR)))**	**R(Q(R(QR)))**	**R(Q(R(QR)))(QR)**	**R(Q(R(QR)))(QR)**	**R(Q(R(QR)))(QR)**	**R(Q(R(QR)))(QR)**	**R(Q(R(QR)))(QR)**	**R(Q(R(QR)))(QR)**

(SZ6)	**24 HOURS**	**48 HOURS**	**72 HOURS**	**96 HOURS**	**120 HOURS**	**144 HOURS**	**WEEK 1**	**WEEK 2**
R_{soln} (mΏ)	10.00	10.00	10.00	10.00	10.00	10.00	10.00	10.00
R_{coat} (kΏ)	66.69	25.87	12.47	10.406	9.474	9.158	8.121	6.098
CPE_{coat} (Y_o, nF cm^{-2} s$^{-(1-\alpha c)}$)	1.332	1.488	1.399	1.4	1.577	1.7	1.734	2.0
a_c	0.930	0.952	0.908	0.952	0.952	0.906	0.952	0.952
R_{ox} (kΏ)	–	–	91.36	69.6	57.25	45.63	39.23	31.90
CPE_{ox} (Y_o, µF cm^{-2} s$^{-(1-\alpha c)}$)	–	–	5	14.09	18.2	21.902	27.56	31.646
a_o	–	–	0.799	0.589	0.100	0.630	0.591	0.573
R_{ct} (kΏ)	256.5	241.4	236.6	111.80	98.36	65.21	20.99	20.77
CPE_{dl} (Y_o, µF cm^{-2} s$^{-(1-\alpha c)}$)	10.38	12.89	16.00	12	15.847	17	19	25
a_d	0.952	0.952	0.952	0.955	0.952	0.947	0.952	0.952
CIRCUIT TYPE	**R(Q(R(QR)))**	**R(Q(R(QR)))**	**R(Q(R(QR)))(QR)**	**R(Q(R(QR)))(QR)**	**R(Q(R(QR)))(QR)**	**R(Q(R(QR)))(QR)**	**R(Q(R(QR)))(QR)**	**R(Q(R(QR)))(QR)**

(SM6)	**24 HOURS**	**48 HOURS**	**72 HOURS**	**96 HOURS**	**120 HOURS**	**144 HOURS**	**WEEK 1**	**WEEK 2**
R_{soln} (mΏ)	10.00	10.00	10.00	10.00	10.00	10.00	10.00	10.00
R_{coat} (kΏ)	79.8	35.45	27.93	27.39	25.55	20. 09	19.22	15.85
CPE_{coat} (Y_o, µF cm^{-2} s$^{-(1-\alpha c)}$)	0.97	1	1.2	1.34	1.47	1.49	1.59	1.70
a_c	0.961	0.958	0.963	0.955	0.913	0.936	0.952	0.952
R_{ox} (kΏ)	–	–	100.6787	72.48	61.23	46.88	42.18	39.277
CPE_{ox} (Y_o, µF cm^{-2} s$^{-(1-\alpha c)}$)	–	–	2.616	12.403	14.77	18.70	23.924	41.30
a_o	–	–	0.267	0.882	0.995	0.354	0.647	0.527
R_{ct} (kΏ)	360.0	243.9	240.92	129.90	142.3	79.09	26.24	27.34
CPE_{dl} (Y_o, µF cm^{-2} s$^{-(1-\alpha c)}$)	4.479	8.94	5.669	10.205	12.089	14.557	18.298	20.607
a_d	0.952	0.952	0.952	0.952	0.952	0.801	0.952	0.952
CIRCUIT TYPE	**R(Q(R(QR)))**	**R(Q(R(QR)))**	**R(Q(R(QR)))(QR)**	**R(Q(R(QR)))(QR)**	**R(Q(R(QR)))(QR)**	**R(Q(R(QR)))(QR)**	**R(Q(R(QR)))(QR)**	**R(Q(R(QR)))(QR)**

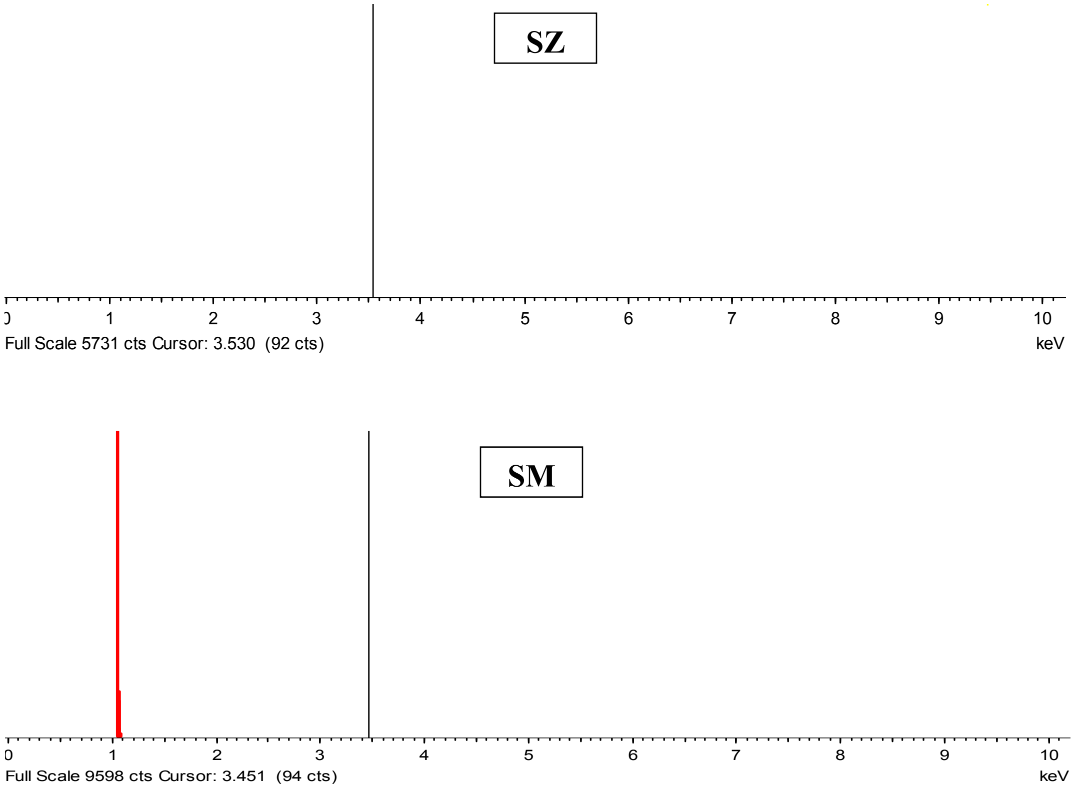

Figure S6. EDX: Elemental composition of SZ and SM sol-gel matrices.

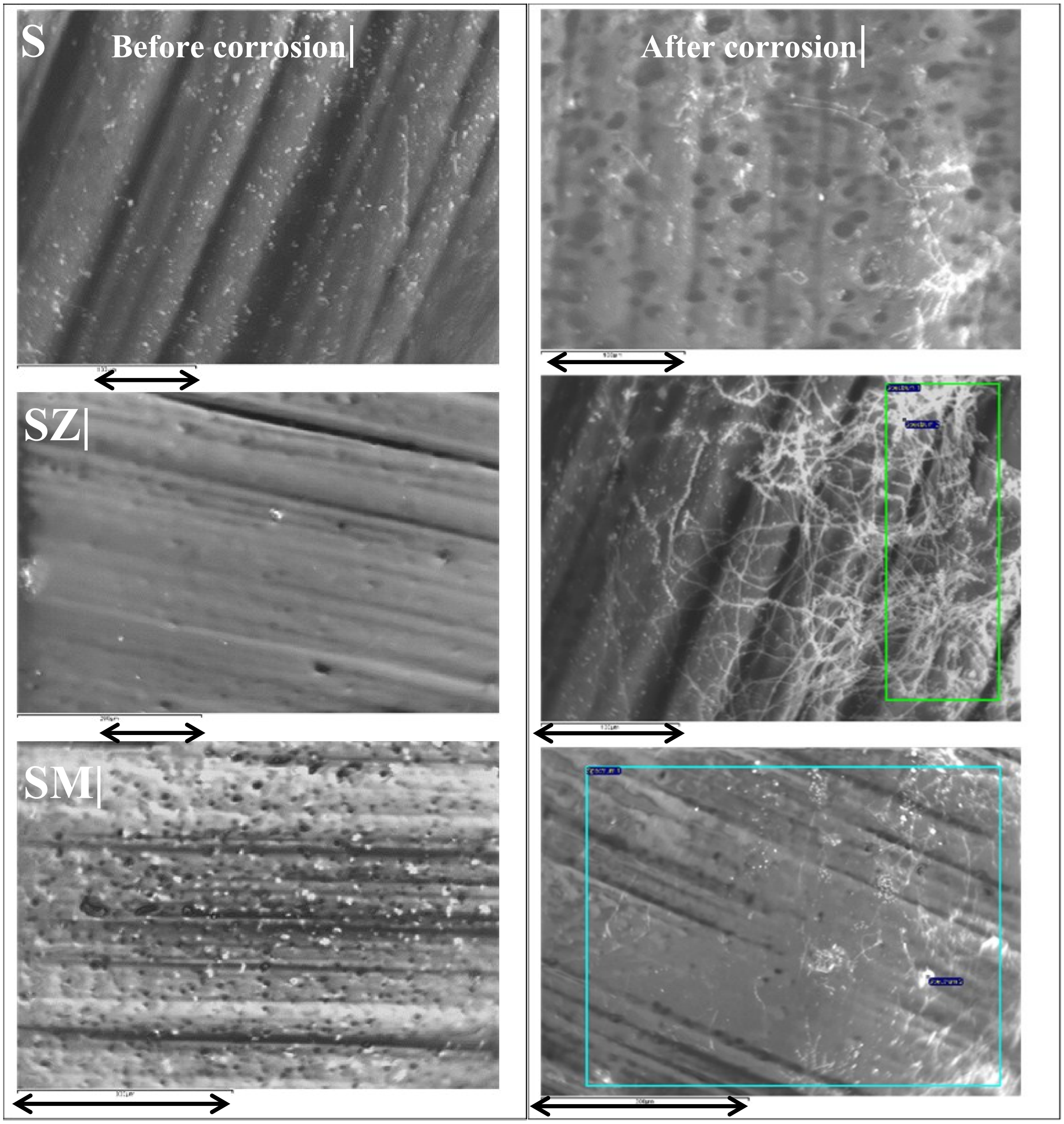

Figure S7. SEM micrographs of the modified (SZ and SM) and unmodified (S) abiotic sol-gel coating showing scale bars (100 µm).